SECED 2023 Conference
Earthquake Engineering & Dynamics for a Sustainable Future
14-15 September 2023, Cambridge, UK

SEISMIC PERFORMANCE OF FIRE-DAMAGED STRUCTURES: PRELIMINARY ANALYSIS OF A 14-STORY CASE STUDY STRUCTURE

Sahin DEDE[1], Tiziana ROSSETTO[2] & Fabio FREDDI[3]

Abstract: *Fires in residential buildings are one of the major and most frequent disasters affecting urban areas. Most fire-damaged buildings are repaired after the fire rather than demolished and replaced. In case of extreme fire events, the decision to repair the building usually involves extensive engineering investigation including materials testing and detailed damage assessment. However, these are often disregarded in case of small to medium size fires, where damage to structural elements may be less visible. In these cases, the repair process focuses on reinstating the aesthetic appearance of the building with limited consideration of how the strength of fire-affected structural elements may have been degraded. But what if the fire-affected building is sited in a seismic area? How will a fire-damaged building perform under seismic loading? The present paper presents an initial study that looks to help answer these questions. The paper evaluates the seismic performance of a typical high-rise reinforced concrete building in Istanbul (of tunnel-form construction), considering several fire damage scenarios. This region is considered for case study purposes due to its high seismic hazard and the high number of residential fires experienced every year (according to the data published by the Istanbul Fire Brigade). The case study structures are modelled in OpenSeesPY, with fire damage modelled considering deterioration in the material properties of the structural components under different scenarios of fire intensity and spread within the building. Nonlinear time history analyses are performed on the undamaged and fire-damaged structures to investigate the changes in the seismic response. The results highlight the increased seismic vulnerability of the fire-damaged structures and provide insights into which fire scenarios most affect the structure's seismic performance.*

Introduction

Frequent residential fires are one of the prominent hazards faced by the building stock in Istanbul, Turkey. Annual data provided in Istanbul Fire Department Statistics (2008-2022) reveal that more than five thousand fire incidents occur each year in residential buildings of Istanbul. In extreme cases, extensive engineering investigation including material testing and detailed damage assessment are usually required to make a decision for the repair of the structure. However, these procedures are often overlooked in case of small to medium size fires, where damage to structural elements may be less visible. In such cases the sole objective of repair is to reinstate the aesthetic apperance of the fire affected unit or the building by usually disregarding the degredation of material properties in structural members. Over-confidence on the fire performance of reinforced concrete, which is by far the dominant construction material in Istanbul, is another reason for the neglect of proper structural assessments after small to medium fires. However, research in structural fire engineering has shown that even short-duration fires could have a significant impact on the behaviour of reinforced concrete members (Ioannou et al., 2022) and therefore, on the structure as a whole. Experimental campaigns have shown that short-duration fires affect the concrete in the core of an element as well as the reinforcing steel through heat transfer (Ioannou et al., 2022; Melo et al., 2022; Demir et al., 2020). Since elevated temperatures have an adverse effect on the properties of concrete (Chang et al., 2006) and steel (Tao et al., 2013), fire-damaged members suffer reduction not only in strength and stiffness but also in ductility and energy dissipation (Ioannou et al., 2022; Melo et al., 2022; Demir et al., 2020). Fire-damaged flexure-controlled shear walls as well experience similar deterioration in their seismic response, as shown by Ni and Briely (2018).

[1] Research Student, EPICentre, University College London, London, U.K. sahin.dede.21@ucl.ac.uk
[2] Professor, EPICentre, University College London, London, U.K.
[3] Dr, EPICentre, University College London, London, U.K.

The degree of strength reduction in structural RC elements due to exposure to small to medium sized fires is not likely to jeopardise the service/daily use of the building, given the safety factors present in the gravity design of buildings. However, they may affect the building response under seismic loading. Istanbul extends parallel to the unruptured segments of the North Anatolian Fault (NFA) that have generated many large magnitude earthquakes in the past, and it is estimated that the probability of occurrence of a magnitude 7.0 or larger earthquake is very high according to Parsons et al. (2000) and Erdik et al. (2003). The seismic performance of fire-damaged buildings has not been studied extensively and could be an important issue for Istanbul, considering the large number of annual fires that occur in the city and the lack of repair and strengthening of fire-damaged buildings.

This paper presents an investigation of the effects of different fire scenarios on the seismic performance of a Turkish RC tunnel-form building. Tunnel-form buildings have been the preferred typology for mass-housing projects in many areas of Istanbul in the last thirty years. They are expected to continue being the main typology for similar projects in the future. In this paper, a 14-storey tunnel form building is modelled in OpenSeesPY (Zhu et al., 2018). Several scenarios of small to medium-sized fires are defined, with increasing severity of fire duration and spread in the building. The reduction in strength and ductility of each fire-exposed structural element is modelled, and the seismic response of the building for each fire scenario is simulated. The post-fire seismic performance of the building is compared with the response in the case of no preceding fire, and the results are discussed. The paper concludes with observations on how the neglect of structural damage from low to medium fires results in an enhanced seismic risk in Istanbul.

Case Study Structure and Finite Element Modelling

Case Study Structure

An existing 14-storey residential building without any active fire protection system and specific protective measurements (e.g. firedoors, protective paint) is selected as the case study to investigate the post-fire seismic response of tunnel-form buildings. Figure 1 shows the plan and elevation view of the case study building. The selected building height, plan and design is representative of hundreds of other mass housing projects across Istanbul.

Figure 1. Floor plan and elevation view of the case study structure

This particular building was selected because of its accessibility for running an ambient vibration measurement scheme to verify the numerical model. Each floor of the building is 27.0 m x 21.6 m in plan dimensions resulting in 520 m^2 of floor area. There are 26 shear walls having 0.2 m thickness on each story, which constitutes 6.44% of the floor area. In addition to shear walls, there are 12 columns in the structural system with three different section dimensions as 0.2 m x 0.2 m, 0.2 m x 0.95m, and 0.2 m x 1.25 m. Vertical structural members are accompanied by 0.15 m thick slabs and 27 beams with varying depths. The total height of the building is 39.2 m, and each story, including the basement enclosed by continuous shear walls, has a height of 2.8 m.

The case study building was constructed in 2010 following the specifications of the Turkish Building Seismic Code 2007 (TBSC 2007). Concrete of compressive strength f_c=30 MPa was

used for all structural components. Steel reinforcement with yield strength f_y=420 MPa was used for the shear wall boundary regions, columns, beams, and slab, whereas steel reinforcement with fy=500 MPa was used for shear wall web regions. All the elements were designed according to the specifications provided for high-ductility members. Although tunnel-form buildings have distinct properties compared to frame-shear wall (dual) systems, the shear walls were designed in compliance with the regulations provided for dual systems due to specific regulations being in place for shear wall buildings. Ground- and first-story shear walls have reinforcement ratios ranging between 0.4%-0.7%, and shear walls in other stories have reinforcement ratios ranging between 0.3%-0.6%. Along the X direction, several shear walls are coupled through conventionally reinforced squat coupling beams having a span-to-depth ratio less than 2.

Finite Element Modelling

A state-of-the-art 3D finite element model of the case study building is achieved by utilising OpenSeesPY. The wide-column analogy is used to model shear walls and wall-like columns where section centroids are connected to neighbouring nodes by stiff, elastic beams. The fiber-based distributed plasticity approach is adopted using '*nonlinearBeamColumn*' to simulate the nonlinear behaviour of shear walls, columns, and beams. Both confined and unconfined concrete properties are represented by the '*Concrete01*' material model, where equations in Mander et al. (1988) are used to estimate the behaviour of confined concrete within the shear wall boundary elements, columns, and beams. The '*Steel02*' material model is adopted for all reinforcing steel. Material nonlinearity is inherently contained in all the material models, whereas, geometric nonlinearity is explicitly taken into consideration by using the '*Pdelta*' coordinate transformation command.

As shear walls are the primary structural member of tunnel-form buildings, their modelling is of key importance for realistically simulating the seismic structural response. Experimental studies and post-earthquake observations have shown that shear walls, especially the thin-sectioned shear walls like that of tunnel-form buildings, mainly suffer from concrete crushing, reinforcement buckling, and reinforcement fracture in earthquakes (Wallace, 2012; Pugh et al., 2015). These damage mechanisms cannot be directly simulated through fiber-based models. To capture these non-simulated failure modes, the material models are modified using the '*MinMax*' command so that they exhibit rapid strength loss after specific strain limits are exceeded. The buckling strain of steel reinforcement is taken to be equal to the crushing strain of the surrounding concrete, defined as the strain at which the concrete experiences an 80% loss of its peak strength. Reinforcement rupture under tension is assumed to occur at 5% tensile strain (Pugh et al., 2015; Gogus and Wallace, 2015). In addition to the non-simulated failure modes, deformation localisation is another phenomenon that needs to be considered if force-based distributed plasticity elements are adopted. Herein, the material regularisation technique recommended by Pugh et al. (2015) is adopted to overcome deformation localisation in shear walls and columns. Lastly, the shear behaviour of shear walls, columns, and beams is defined by means of the '*section Aggregator*' command. A bilinear shear force-shear deformation relationship is defined for each element using the '*Hysteretic*' material. Slabs and peripheral basement walls are modelled as elastic membrane plate elements, and cracked section stiffness reduction factors are applied. Their bending stiffness is seen to reduce by 25% and 50%, respectively, in accordance with common practice (TBSC 2018, ACI 318-14). The structural mass of the system is distributed to the joints at each floor level based on the dead loads, live loads, and self-weight of the system.

The modelling methodologies used for the structural members have already been validated in the literature. However, the finite element model herein is a detailed 3D representation of a complex high-rise structure. In order to verify the appropriateness of the numerical model, ambient vibration measurements of the actual building were conducted to identify its dominant periods of vibration. Due to space limitations, the details of the signal processing are not provided here, but Fourier spectral analysis of these recorded low-amplitude data shows that the first three fundamental periods are between 1.7 and 2.0 Hz. The first mode is dominated by torsion, whereas the second and third modes are dominated by the translational response and have almost the same frequency. Table 1 presents the periods associated with the first three modes of the finite element model with and without stiffness modification factors applied. Comparison of the measured versus modelled periods of vibration is conducted with the latter model, (since ambient vibration measurement captures only the elastic response under low-amplitude motions), and shows a good correspondence.

Mode	Finite element model without cracked section stiffness	Finite element model with cracked section stiffness
First Mode (Torsional)	0.52 s (1.92 Hz)	0.64 s (1.56 Hz)
Second Mode (Translational X)	0.50 s (2.00 Hz)	0.58 s (1.72 Hz)
Third Mode (Translational Y)	0.48 s (2.08 Hz)	0.55 s (1.82 Hz)

Table 1. Modal periods of the case study structure

Implementation of Fire Damage

As mentioned above, nonlinearity in the finite element model of the case study is simulated through fiber-based elements. The key component in this modelling methodology is the material definition since the constitutive relationship of uniaxial material models at each integration point governs the nonlinear response. In order to represent the post-fire situation, the material properties were altered to represent the deterioration in response due to fire. Herein, the framework proposed by Ioannou et al. (2022) is adopted to represent the post-fire material behaviour. Ioannou et al. (2022) investigated the post-fire cyclic behaviour of pre-code RC columns and presented experimentally validated material models for use in numerical analyses. Although Ioannou et al. (2022) focus on 0.30 m square pre-code columns, their confined and unconfined concrete models are sufficient for a preliminary investigation of the case study building, as the shear walls modelled are very thin (0.20 m) and can be assumed to fully transfer heat from one side of the element to the other. Hence, the post-fire material properties are applied to shear walls and columns in each room using the same coefficients as proposed in Ioannou et al. (2022) to represent post-fire strength, ductility, and stiffness changes. A uniform heat distribution is assumed within each room and apartment (BS EN 1991. 1-2; Buchanan and Abu, 2017). Only the vertical load-bearing elements were subjected to degradation within the scope of this preliminary work, as these elements are the primary members determining structural stability. Stress-strain relationships and applied strain limits for all the fire-affected members are revised to reflect the degradation in material properties. Additionally, the shear force-shear deformation relationships are updated considering the fire damage on the section. All these alterations are conducted in accordance with the fire scenarios presented in the next section.

Seismic Performance Assessment of Fire-Damaged Structures

Five different fire damage scenarios in addition to the undamaged state are considered for the investigation of the post-fire seismic response of the case study structure. This results in six versions of the finite element model being analysed. For preliminary research purposes, the fire hazard is not modelled explicitly; therefore, parameters affecting the fire dynamics, e.g., ventilation and thermal properties, are not provided. It is assumed that the building has undergone a fire incident at some point during its service life and has only undergone aesthetic renovation without any structural repair. Figure 2 shows the flats used as the basis for defining the scenarios. Each flat has a 100m^2 floor area and has neither an active fire protection system nor any fireproof measures.

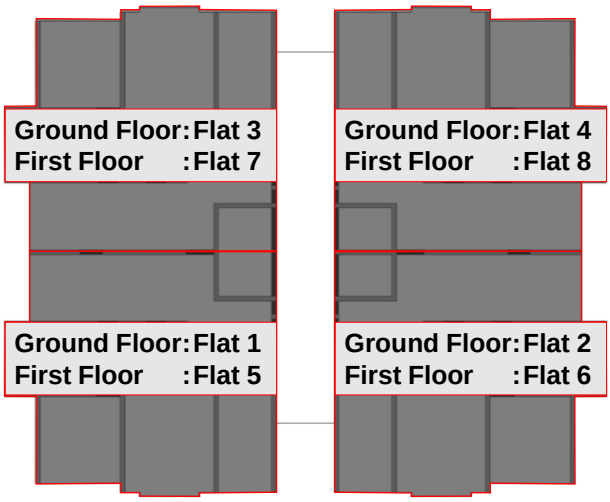

Figure 2. Flat numbers

In this study, the five fire scenarios are defined assuming an increase in fire intensity and progressive fire spread. Table 2 presents the scenarios and fire damage considered in each flat for each scenario. Scenario 0 refers to the undamaged state of the building. In Scenario 1, a 30-minute fire incident is assumed to occur at the ground floor of the building, causing damage to the structural elements of Flat 1. In scenario 2, the fire in Flat 1 has become more intense and has spread to two adjoining flats. A similar rationale for fire spread is applied for the subsequent scenarios until, in Scenario 5, all flats in both the ground and first storey have sustained a 90-minute fire.

Scenario	**Ground Floor**				**First Floor**			
	Flat 1	**Flat 2**	**Flat 3**	**Flat 4**	**Flat 5**	**Flat 6**	**Flat 7**	**Flat 8**
0	-	-	-	-	-	-	-	-
1	30	-	-	-	-	-	-	-
2	60	30	30	-	-	-	-	-
3	90	60	60	30	30	-	-	-
4	90	90	90	60	60	30	30	-
5	90	90	90	90	90	90	90	90

Table 2. Scenario fire damages as minutes

It is important to state that, the durations herein do not refer to the exact time span of the fire event. Instead, they refer to the quantified effect of fire on material properties as per the experimental campaign presented by Melo et al. (2022) and used by Ioannou et al. (2022) for the fire damage modelling. The fire durations in these studies were defined according to the ISO-834 time-temperature curves, which are the primary practice in fire rating tests and constitute a common language in fire engineering; however, they are not representative of real fires (Buchanan and Abu, 2017). Tables 3 and 4 present the post-fire material properties as a proportion of the undamaged material properties used to model the effects of the 30 mins, 60 mins, and 90 mins of fire damage. These coefficients are used to modify the material properties of the structural members exposed to each fire duration in each fire scenario.

Fire Damage as Minutes	f_{cy}		ε_{cy}		f_{cu}		ε_{cu}	
	Cover Concrete	Core Concrete	Cover Concrete	Core Concrete	Cover Concrete	Core Concrete	Cover Concrete	Core Concrete
No prior damage	1.00	1.00	1.00	1.00	1.00	1.00	1.00	1.00
30	0.64	0.90	1.95	1.00	0.62	0.90	1.06	1.03
60	0.55	0.80	2.50	1.25	0.53	0.81	1.15	1.05
90	0.45	0.71	3.05	1.50	0.44	0.71	1.25	1.07

Table 3. Coefficients used to reflect post-fire concrete material properties

Fire Damage as Minutes	f_{sy}	E_s (MPa)	f_{su}	ε_{su}	b_s
No prior damage	1.00	1.00	1.00	1.00	1.00
30	1.00	1.00	1.00	1.03	1.00
60	0.93	0.98	0.94	0.97	1.04
90	0.87	0.97	0.88	0.91	1.09

Table 4. Coefficients used to reflect post-fire reinforcing steel material properties

Dynamic time-history analyses of the case study building model, modified for each scenario, are carried out using a single set of ground motion records. The chosen acceleration records correspond to data recorded at Yarimca station during the M_w=7.4 Kocaeli earthquake of the 17th August, 1999. This event is one of the most recent large events that have occurred along the NAF, and this ground motion is considered to be representative of the fault characteristics. The record was scaled by a factor of 2.4, so as not to fall below the site design spectral acceleration values between the periods $0.2T_1$-$2.0T_1$ (TBSC 2007). The adopted ground motion record and its corresponding spectral response can be seen in Figure 3, along with the spectrum used to design the case study structure. Nonlinear time history analyses are conducted by applying two horizontal components on the orthogonal directions of the 3D finite element model.

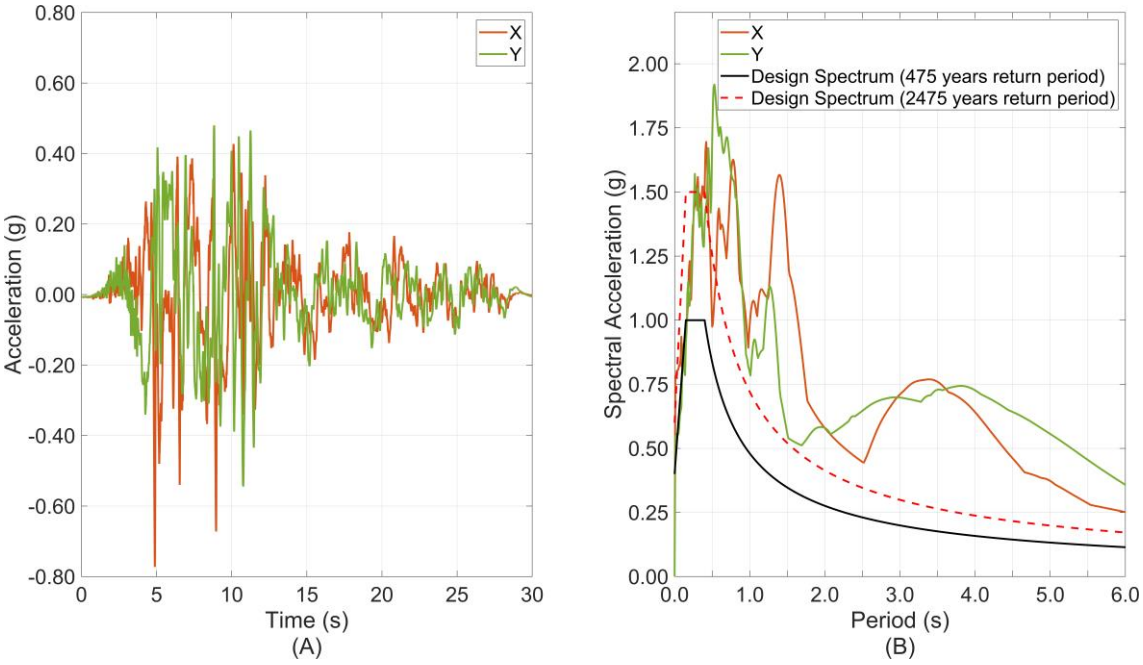

Figure 3. M_w = 7.4 Kocaeli earthquake (A) acceleration record (B) response spectra

Results

Figure 4 to Figure 7 and Table 5 compare the results obtained from the undamaged case to those obtained from post-fire damage scenarios. Variations of the modal properties of the structural model for the different fire scenarios are presented in Table 5. Displacement response histories of each case are provided in Figure 4 and Figure 5 separately for each direction, together with the 2D planar motion on orthogonal directions. Lastly, Figure 6 and Figure 7 compare the maximum and residual inter-story drift ratios (IDR) calculated for each scenario.

Scenario	First Mode (Torsion)		Second Mode (X)		Third Mode (Y)	
	T (s)	Γ (%)	T (s)	Γ (%)	T (s)	Γ (%)
0	0.63	69.1	0.58	72.4	0.54	68.4
1	0.69	68.5	0.58	72.4	0.55	68.3
2	0.70	68.4	0.59	72.2	0.56	68.2
3	0.71	68.2	0.60	71.9	0.57	67.9
4	0.72	68.1	0.62	71.6	0.59	67.6
5	0.73	68.0	0.63	71.4	0.61	67.0

Table 5. Comparison of modal parameters for each scenario

From Table 5, it is observed that even the most severe scenario does not result in more than 10% period lengthening. It is also seen that even the asymmetric fire spread scenarios, e.g., Scenario 3, do not significantly impact the torsional mode. Based on this specific case, it can be said that the post-fire state of the building does not have a significant effect on the modal properties of the structure when compared to the undamaged state. There is a steady decrease in the modal mass participation factors, but this is not significant. These observations suggest that, in practice, fire damage at the local level (even spread across two storeys) may not be detectable using methods like global structure ambient vibration measurement.

It is observed in Figure 5 that the building is more ductile along its long direction (X) compared to its short direction, and tends to lean more in the Y direction under this specific ground motion for the fire damage scenarios. It is observed that the building's response is almost unchanged in Scenarios 1 and 2 as compared to the undamaged case (Scenario 0). From Scenario 3 onwards, the structure exhibits severe oscillations and suffers residual displacements in different directions.

The displacement histories in Figure 4 and Figure 5 show that the asymmetric fire damage of Scenario 3 creates the most severe effect along the X direction. It is evident from Figure 4 that the building cannot recover its original position in Scenario 3, which has medium severity but the largest asymmetry. The amplified response in Scenario 3 may be attributed to the dominance of the torsional response in this building typology. Along the Y direction, Scenario 3 does not result in the largest damage but does cause a residual displacement in the opposite direction to the other cases, which may be attributed to the asymmetric loading condition.

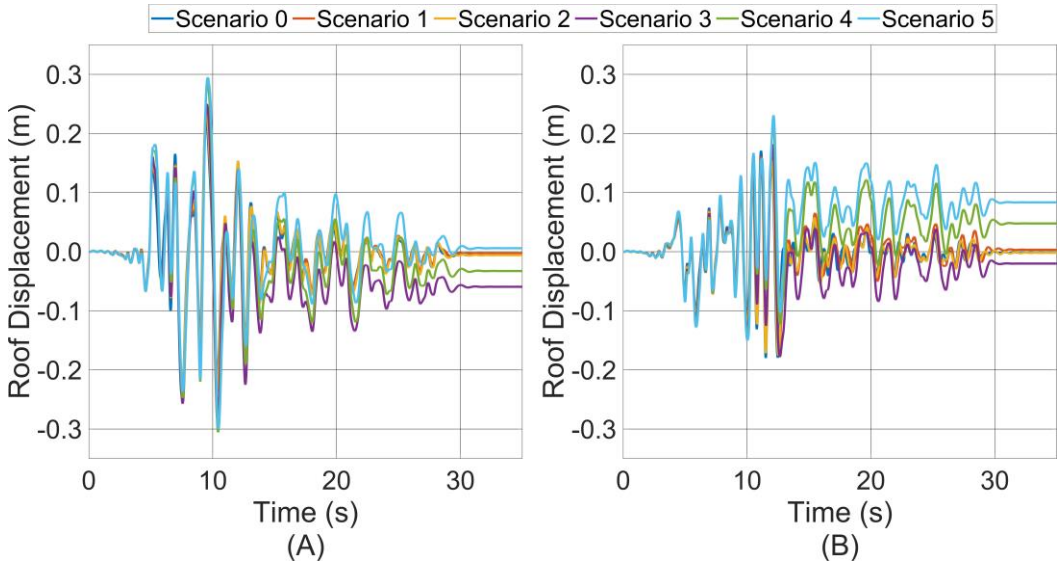

Figure 4. Displacement response of each scenario at a central point on roof. (A) X direction (B) Y direction.

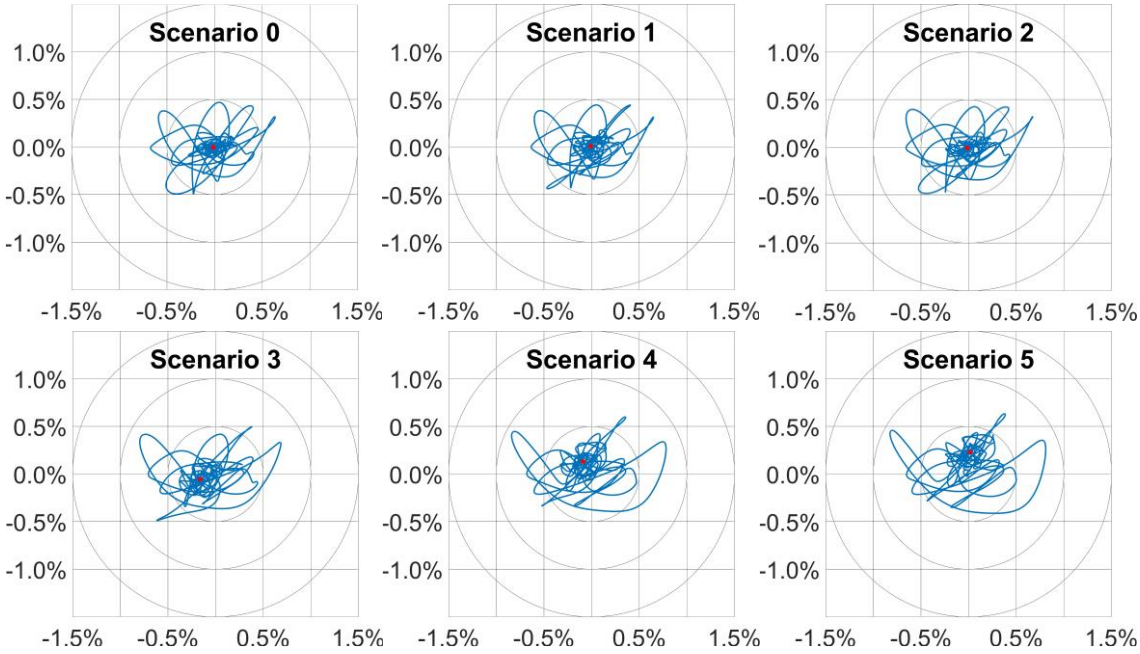

Figure 5. Planar display of displacement response at a central point on the roof proportioned to the building height above the ground. X direction is the horizontal axis and Y direction is the vertical axis. Red dot indicates the final displacement of the point.

The ground floor of the building, the story between 0.0 and 2.8 meters, at Scenario 0, suffers the largest IDRs, as shown in Figure 6. This soft-story response of the ground floor is also preserved in Scenario 1 and 2. However, from Scenario 3 onwards, the soft-story response is not only shifted to the first floor but also amplified. These observations are also supported by Figure 7, as residual IDRs are prominent on the first floor, the story between 2.8 and 5.6 meters.

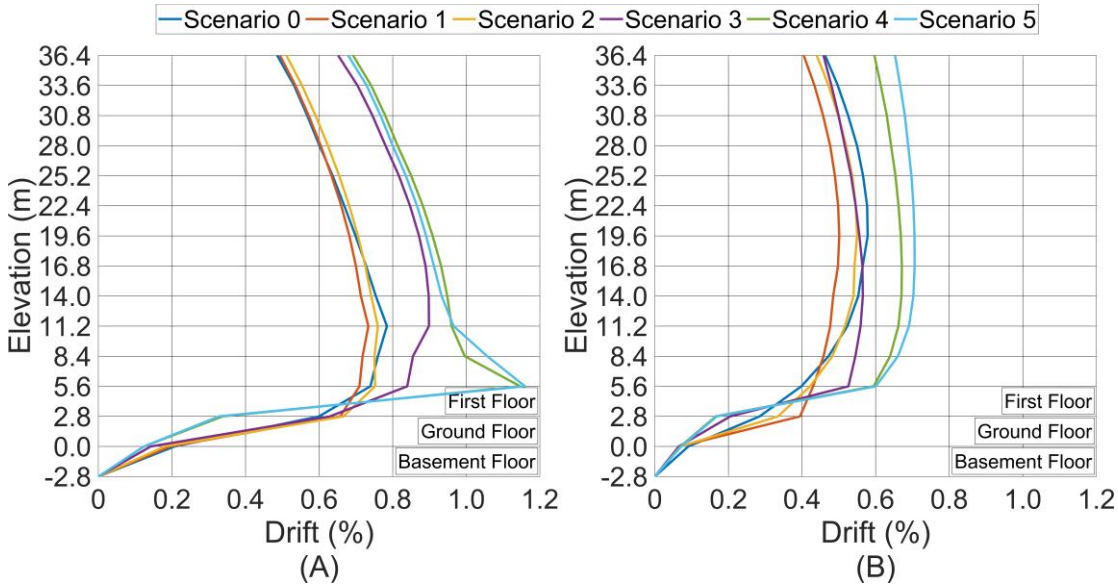

Figure 6. Maximum interstory drift ratios obtained at a central point of each floor for each scenario. (A) X direction (B) Y direction.

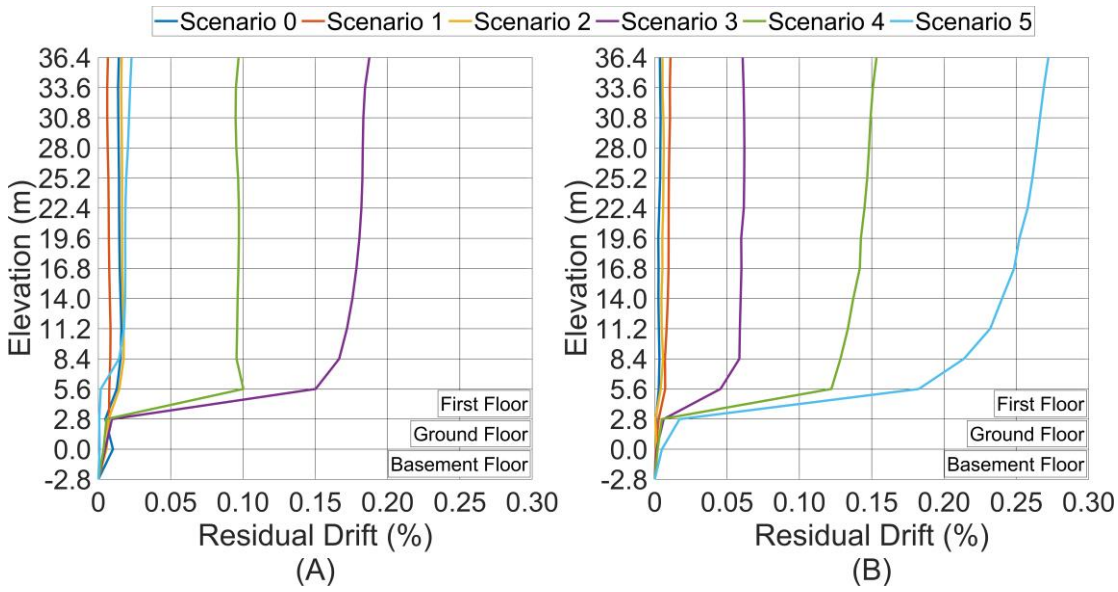

Figure 7. Residual interstory drift ratios obtained at a central point of each floor for each scenario. (A) X direction (B) Y direction.

Conclusion

This study investigates the post-fire seismic response of a 14-storey tunnel-form building in Istanbul through several scenarios of small to medium-sized fires, with increasing severity of fire duration and spread in the building. Fire severity is considered at material and section levels by altering strength, stiffness, and ductility parameters to represent the fire-damaged properties.

Modal analysis results show that fire damage at the local level, even two storeys suffered damage, does not considerably affect the natural vibration periods and modal mass participation. The fire damage might not be measurable using ambient vibration measurement if conducted only at roof level, as the model periods for damaged and undamaged structures are similar. Buildings that experienced small to medium size fires might not be distinguished if damage history is unknown.

Progressive fire spread and increasing severity of fire, as expected, results in more severe oscillations, higher residual displacements and amplified interstory drift ratios. But an important observation here is that the duration and spread of fire do not proportionally increase the seismic vulnerability of the building as the most asymmetric scenario led to the most severe effects compared to more extensive fire damage scenarios in one direction. This observation suggests that asymmetry of the damage distribution and structural configuration also have an influence on the post-fire seismic response.

The neglect of structural damage from low to medium size fires results in an enhanced seismic risk in Istanbul, as the outcomes of this preliminary investigation show the increased seismic vulnerability of fire-damaged buildings. A more detailed representation of the thermal response of fire-exposed structural members and advanced modelling of fire behaviour are needed to better understand the important consequences of fire on seismic performance.

References

Istanbul Fire Department Statistics (2008-2022). Istanbul Metropolitan Municipality, Turkey.

Ioannou, I., Rossetto, T., Rush, D. and Melo, J., 2022. Simplified model for pre-code RC column exposed to fire followed by earthquake. Scientific reports, 12(1), p.8980.

Melo, J., Triantafyllidis, Z., Rush, D., Bisby, L., Rossetto, T., Arêde, A., Varum, H. and Ioannou, I., 2022. Cyclic behaviour of as-built and strengthened existing reinforced concrete columns previously damaged by fire. Engineering Structures, 266, p.114584.

Demir, U., Goksu, C., Unal, G., Green, M. and Ilki, A., 2020. Effect of fire damage on seismic behavior of cast-in-place reinforced concrete columns. Journal of Structural Engineering, 146(11), p.04020232.

Chang, Y.F., Chen, Y.H., Sheu, M.S. and Yao, G.C., 2006. Residual stress–strain relationship for concrete after exposure to high temperatures. Cement and concrete research, 36(10), pp.1999-2005.

Tao, Z., Wang, X.Q. and Uy, B., 2013. Stress-strain curves of structural and reinforcing steels after exposure to elevated temperatures. Journal of Materials in Civil Engineering, 25(9), pp.1306-1316.

Ni, S. and Birely, A.C., 2018. Post-fire seismic behavior of reinforced concrete structural walls. Engineering Structures, 168, pp.163-178.

Parsons, T., Toda, S., Stein, R.S., Barka, A. and Dieterich, J.H., 2000. Heightened odds of large earthquakes near Istanbul: an interaction-based probability calculation. Science, 288(5466), pp.661-665.

Erdik, M., Aydinoglu, N., Fahjan, Y., Sesetyan, K., Demircioglu, M., Siyahi, B., Durukal, E., Ozbey, C., Biro, Y., Akman, H. and Yuzugullu, O., 2003. Earthquake risk assessment for Istanbul metropolitan area. Earthquake Engineering and Engineering Vibration, 2, pp.1-23.

Zhu, M., McKenna, F. and Scott, M.H., 2018. OpenSeesPy: Python library for the OpenSees finite element framework. SoftwareX, 7, pp.6-11.

Turkish Building Seismic Code (2007). The Ministry of Public Works and Settlement, Ankara, Turkey.

Mander, J.B., Priestley, M.J. and Park, R., 1988. Theoretical stress-strain model for confined concrete. Journal of structural engineering, 114(8), pp.1804-1826.

Wallace, J.W., 2012. Behavior, design, and modeling of structural walls and coupling beams—Lessons from recent laboratory tests and earthquakes. International Journal of Concrete Structures and Materials, 6, pp.3-18.

Pugh, J.S., Lowes, L.N. and Lehman, D.E., 2015. Nonlinear line-element modeling of flexural reinforced concrete walls. Engineering Structures, 104, pp.174-192.

Gogus, A. and Wallace, J.W., 2015. Seismic safety evaluation of reinforced concrete walls through FEMA P695 methodology. Journal of Structural Engineering, 141(10), p.04015002.

Turkish Building Seismic Code (2018). Disaster and Emergency Presidency, Ankara, Turkey.

ACI (2014) ACI 318-14: Building code requirements for reinforced concrete. American Concrete Institute, Farmington Hill, USA.

Buchanan, A.H. and Abu, A.K., 2017. *Structural design for fire safety*. John Wiley & Sons.

BS EN 1991. 1-2: 2002 Eurocode 1: Actions on structures—Part 1-2: General actions—Actions on structures exposed to fire. British Standards.